Eur. Phys. J. Special Topics **223**, 1259–1264 (2014)

DOI: 10.1140/epjst/e2014-02189-7

THE EUROPEAN PHYSICAL JOURNAL SPECIAL TOPICS

Regular Article

An instability at the edge of a tissue of collectively migrating cells can lead to finger formation during wound healing

J. Zimmermann[1,b], M. Basan[2,b], and H. Levine[1,a]

[1] Center for Theoretical Biological Physics, Rice University, Houston, Texas, USA
[2] Center for Theoretical Biological Physics, University of California at San Diego, La Jolla, California, USA

Received 9 January 2014 / Received in final form 14 April 2014
Published online 12 June 2014

Abstract. In wound healing assays, a monolayer of epithelial cells is allowed to migrate onto empty surface area. When the motile cells close the artificial wound, the edge of the tissue does usually not move uniformly but characteristic fingerlike protrusions are observed. We model the collectively moving cells as a system of self-propelled particles using the Toner-Tu equations for an active fluid. A linear stability analysis of perturbations at the tissue edge reveals an instability in the disordered nonmoving state. The instability is purely due to spontaneous motility and velocity alignment between cells. It can account for finger formation in wound healing experiments.

1 Introduction

The term "active matter" is used to describe collectives of particles that use energy to propel themselves forward and that interact with each other due to mechanical forces. The individual particles can be living or nonliving, and systems can extend over very different length scales from several microns to many hundreds of meters. Some examples of active matter systems that have attracted interest are vibrated rods, motility assays consisting of cytoskeletal filaments and motor proteins, swimming bacteria, migrating cells, swarms of insects or birds, schools of fish and groups of humans [1]. These systems exhibit a variety of interesting non-equilibrium properties, such as the emergence of large scale polarity and/or the formation of ordered macroscopic patterns [1].

An interesting question is, to what extent those systems can be described by a simple unified continuum theory. One of the first studies of emergent behavior was carried out by Vicsek et al. [2], where a set of rules was assigned to account for motion of the individuals and for interaction between neighbors in the swarm. Vicsek et al. observed a transition from a disordered state at low density or high noise strength to an ordered polar state at high density or low noise strength. Toner and Tu [3–5]

[a] e-mail: herbert.levine@rice.edu
[b] Those authors contributed equally to this work.

developed a continuum theory that described the large scale behavior of the model system in terms of macroscopic variables. Following the classification in Ref. [1], the Toner-Tu hydrodynamic equations are considered a "dry" model, with friction with the substrate dominating and the total momentum not being conserved. In contrast, the total momentum is conserved in "wet" systems since they are dominated by viscosity [1]. Wet systems are accounted for by the theory of active gels [6,7], which was primarily developed to describe fluids of filaments driven by motor proteins.

Our calculations in this paper are motivated by the collective migration of epithelial cells. During wound healing, cells not only divide, but start moving actively to close the wound, while they are attached to each other at cell-cell junctions through trans-membrane proteins called cadherins. *In vitro*, wound healing is studied by growing cells into a confluent monolayer covering the substrate, and then either by removing cells, e.g. by scratching [8], or by unmasking free surface area, e.g. by removing obstacles that prevent cell growth [9,11]. Cells start filling the void space. Characteristically, the leading edge of the monolayer does not move uniformly, but fingerlike protrusions form when the artificial wound closes [9]. Simulations of the wound healing process showed that finger formation depends on cell-cell adhesion [10], and is an emergent phenomenon that requires interaction between cells. Since collectively migrating cells are tightly adhered to the substrate, they are well described by the Toner-Tu continuum equations. In the following, we show that the formation of fingerlike protrusions can be accounted for by an undulation instability at the edge of a film of active fluid.

Instability is a common theme in the theory of active matter [1]. A stability analysis of density and polarity fluctuations in the bulk of a dry Toner-Tu type fluid shows that the disordered isotropic state is always stable at low densities [1]. However, various instabilities, e.g. giant density fluctuations, exist in the bulk in the polar state [5]. Instabilities at interfaces have been studied in wet models. When the upper surface of a thin active gel film is free to undulate, instabilities and wave formation are observed [12–14]. To our knowledge, a linear stability analysis of a 2d interface in a dry system is presented here for the first time.

2 Governing equations

Our model tissue is described by the following set of equations [4]:

$$\bigtriangledown \cdot \mathbf{v} = 0, \tag{1}$$

$$\eta \bigtriangledown^2 \mathbf{v} - \bigtriangledown p + \alpha \mathbf{v} - \beta |\mathbf{v}|^2 \mathbf{v} = \rho \left(\frac{\partial \mathbf{v}}{\partial t} + \lambda_1 (\mathbf{v} \cdot \bigtriangledown) \mathbf{v} \right), \tag{2}$$

with the velocity field $\mathbf{v}$ and the pressure p. The continuity equation (1) implies that the tissue flow is incompressible, and cells do not divide or die. This is a reasonable approximation due to the fact the division rate is low in wound healing experiments, and if cells divide, they do so mainly in the center of the monolayer [9]. The constant density ρ also does not allow for density fluctuations. One could include compressibility effects, but then the model would have to be extended to explicitly include the coexistence of high and low density phases. This would require explicit consideration of cell-cell adhesion in the bulk equation; see for example the work of Khain and Sander [15].

Equation (2) accounts for the force balance in the tissue. In addition to the advection terms on the right hand side, the viscosity η and the pressure term are reminiscent of a Navier-Stokes equation for conventional fluids. The coupling of the velocity to the active motility of the cells is described by a negative friction with the

coefficient α. Friction with the substrate is accounted for by the fourth term on the left hand side with the coefficient β. The coefficient λ_1 expresses the fact that our system is not constrained by Galilean invariance since the total momentum is not conserved. However, our system operates at low Reynolds numbers (small length scales, slow flow), and viscous forces are much larger than inertial forces. Therefore, we set the right hand side of Eq. (2) equal to zero in the following. Together with appropriate boundary conditions (see Sect. 3), the system of equations (1), (2) can describe motile cells in a wound healing assay.

We consider the two dimensional geometry shown in Fig. 1A. The tissue is located between $x = -L$ and $x = 0$, and is homogeneous in y-direction in the unperturbed case. The system of Equations (1), (2) has a moving and a nonmoving solution, given by $v_x = v_0$, with $v_0 = \sqrt{\alpha/\beta}$ and $v_0 = 0$, respectively. The pressure $p = p_0$ is constant. We assume that the tissue is constrained at $x = -L$ by a wall, which is comoving with the unperturbed solution. The tissue edge at $x = 0$ can be described by a curve $h(y, t)$. In the following section, we analyze the linear stability of small perturbations δh of this interface.

3 Stability analysis of tissue edge

We introduce perturbations to the moving and nonmoving solution, $\mathbf{v} = v_0\hat{\mathbf{x}} + \delta\mathbf{v}$ and $p = p_0 + \delta p$. The perturbations can be expressed in terms of normal modes, i.e., $\delta\mathbf{v} = (\delta\tilde{v}_x\hat{\mathbf{x}} + \delta\tilde{v}_y\hat{\mathbf{y}})\exp(iqy + \omega t + k(x - v_0t))$ and $\delta p = \delta\tilde{p}\exp(iqy + \omega t + k(x - v_0t))$. Substituting those into Eq. (1) yields

$$\delta v_x = -\frac{iq}{k}\delta v_y. \tag{3}$$

The linearized x- and y-component of Eq. (2) read

$$\eta(k^2 - q^2)\delta v_x - k\delta p + \alpha\delta v_x - 3\beta v_0^2\delta v_x = 0, \tag{4}$$

$$\eta(k^2 - q^2)\delta v_y - iq\delta p + \alpha\delta v_y - \beta v_0^2\delta v_y = 0. \tag{5}$$

Imposing the condition that the system of Eqs. ((3), (4), (5)) has a non-zero solution, we can calculate the wavenumber k as

$$\begin{aligned} k_\pm^2 &= q^2 + \frac{1}{2\eta}(-\alpha + \beta v_0^2) \pm \sqrt{\frac{1}{4\eta^2}(-\alpha + \beta v_0^2)^2 - q^2 2\beta v_0^2/\eta}, \\ k_1 &= +\sqrt{k_+^2}, \quad k_2 = -\sqrt{k_+^2}, \quad k_3 = +\sqrt{k_-^2}, \quad k_4 = -\sqrt{k_-^2}. \end{aligned} \tag{6}$$

Hence, the general perturbed solution reads

$$\begin{aligned} v_x &= v_0 + \sum_{n=1}^{4} A_n \mathrm{e}^{iqy+\omega t}\mathrm{e}^{k_n(x-v_0t)}, \\ v_y &= \sum_{n=1}^{4} B_n \mathrm{e}^{iqy+\omega t}\mathrm{e}^{k_n(x-v_0t)}, \\ p &= p_0 + \sum_{n=1}^{4} C_n \mathrm{e}^{iqy+\omega t}\mathrm{e}^{k_n(x-v_0t)}. \end{aligned} \tag{7}$$

The coefficients B_n and C_n can be expressed as functions of A_n by inserting those expressions into Eqs. (1), (2).

The moving tissue edge is described by a curve $h(y,t)$. We also perturb this interface, so that it can be expressed as $h(y,t) = \delta h \exp(iqy + \omega t)$ in a frame of reference moving with velocity v_0. We then impose the following boundary conditions. The perturbations vanish at the back of the tissue ($x = v_0 t - L$): $v_x = v_0$, $v_y = 0$, and the following conditions hold at the leading edge ($x = v_0 t + h(y,t)$):

- No transverse stress: $\partial v_x/\partial y + \partial v_y/\partial x = 0$,
- The normal stress equals the surface tension: $2\eta \partial v_x/\partial x - p = \gamma \partial^2 h/\partial y^2$,
- The motion of the boundary equals the flow velocity at the boundary: $\partial h/\partial t = \delta v_x$.

Inserting the general expressions of Eq. (7) into the boundary conditions yields the linear system of equations

$$\begin{aligned}
&\sum_{n=1}^{4} A_n \mathrm{e}^{-k_n L} = 0,\\
&\sum_{n=1}^{4} -\frac{k_n}{iq} A_n \mathrm{e}^{-k_n L} = 0,\\
&\sum_{n=1}^{4} -(q^2 + k_n^2) A_n = 0,\\
&\sum_{n=1}^{4} \frac{-\eta(k_n^2 + q^2) + \alpha - 3\beta v_0^2}{k_n} A_n = \gamma\, q^2 \delta h,\\
&\sum_{n=1}^{4} A_n = \omega \delta h.
\end{aligned} \tag{8}$$

We can calculate ω as a function of q by again solving the characteristic equation. The result is shown in Fig. 1B–D.

4 Discussion and Conclusion

We find that the moving solution is stable for all tissue width L (Fig. 1B). In contrast, the nonmoving solution is unstable for all relevant tissue width above one cell diameter (Fig. 1C and D). Alignment of the velocities of actively moving cells leads to instability of the moving and stability of the nonmoving state. If cells are initially stationary, small fluctuations in the velocity can lead to alignment of neighboring cells, collective motion in some random direction, and swirl formation. When swirls impinge on the tissue edge, finger-like protrusions can form [9]. In contrast, velocity alignment dampens fluctuations when cells already have a uniform velocity, and the tissue edge moves uniformly.

The form of the instability is somewhat unusual. In the limit we have considered, which completely neglects the time derivative terms on the right hand side of the governing equation, the growth rate is unbounded. This means that the time-evolution is actually ill-defined, and a full treatment must include those terms. The origin of this

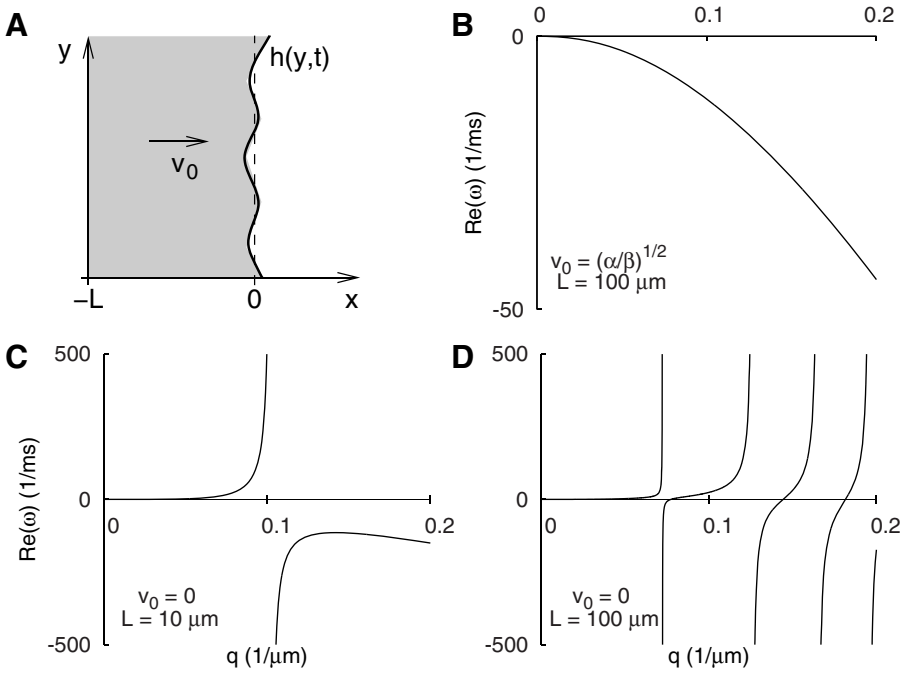

Fig. 1. (A) Sketch of the tissue geometry. (B–D) Real part of ω as a function of the wave number q. (B) For the moving solution with $L = 100\,\mu$m. The moving solution is stable for all L. (C) For the nonmoving solution with $L = 10\,\mu$m. (D) For the nonmoving solution with $L = 100\,\mu$m. The nonmoving solution is unstable, and some modes grow infinitely fast. The number of poles in ω increases with increasing tissue length L. Parameters are: $\eta = 10^4\,\mathrm{Pa\,s}$ [16,17], $\gamma = 10^9\,\mathrm{Pa}\,\mu\mathrm{m}$ [18], $\alpha = 60\,\mathrm{Pa\,s}/\mu\mathrm{m}^2$, $\beta = 10^7\,\mathrm{Pa\,s}^3/\mu\mathrm{m}^4$.

behavior can be seen in the expression for the wave vectors $k_\pm^2$. When $v_0 = 0$, the four roots are $k = \pm q$ and $k = \pm i\sqrt{\alpha/\eta - q^2}$. The fact that the two middle roots (in terms of ordering based on $\mathrm{Re}(k)$) have equal real parts for sufficiently small q means that in the $L \to \infty$ limit, the boundary conditions can be satisfied for all values of ω. The analog for this fourth-order system is the continuous (positive energy) eigenvalue spectrum of a Schroedinger operator, as discussed e.g. in [19]. In particular, the signature of this behavior in a finite-sized box is the type of discontinuous behavior of ω versus q seen in Fig. 1C and D.

The results of our stability analysis are in agreement with simulations [10] and experimental data. In wound healing assays, cells are typically grown into a confluent layer, before some cells or obstacles are removed, and cells are allowed to invade the empty space. Hence, cells are in a nonmoving state before they start closing the artificial wound. Finger formation at the wound edges is observed in those experiments [9], reflecting the instability of the nonmoving state in our calculation. In other types of experiments, a small number of cells is plated on a substrate, and they start forming a monolayer [20]. In those growing circular cell colonies, cells divide mainly in the center. Only mild undulations at the tissue edge are observed, since cells exhibit a velocity normal to the tissue edge during spreading, which corresponds to the stability of the moving state.

It has been speculated that specialized leader cells are located at the tips of fingers, and drag the cells behind them [9]. Inclusion of leader cells in mathematical models could explain finger formation [21,22]. Although we do not exclude that cells

at the edge have different properties from cells in the bulk, our results show that an instability can drive finger formation. The instability stems purely from coordinated cell motility and is independent of leader cells. We also do not have to consider density fluctuations in our stability analysis. The instability found here is likely not only relevant for collective cell migration, but might describe the behavior at interfaces and finger formation in other systems such as swarms or herds of birds, insects or ungulates.

This work was supported by the NSF Center for Theoretical Biological Physics (NSF grant No. PHY-1308264), and by NSF grant DMS-1068869. HL is also supported by CPRIT Scholar program of the State of Texas.

References

1. M.C. Marchetti, J.F. Joanny, S. Ramaswamy, T.B. Liverpool, J. Prost, M. Rao, R.A. Simha, Rev. Mod. Phys. **85**, 1143(47) (2013)
2. T. Vicsek, A. Czirok, E. Ben-Jacob, I. Cohen, O. Shochet, Phys. Rev. Lett. **75**, 1226 (1995)
3. J. Toner, Y. Tu, Phys. Rev. Lett. **75**, 4326 (1995)
4. J. Toner, Y. Tu, Phys. Rev. E **58**, 4828 (1998)
5. J. Toner, Y. Tu, S. Ramaswamy, Ann. Phys. **318**, 170 (2005)
6. K. Kruse, J.F. Joanny, F. Jülicher, J. Prost, K. Sekimoto, The Eur. Phys. J. E **16**, 5 (2005)
7. F. Jülicher, K. Kruse, J. Prost, J.-F. Joanny, Phys. Rep. **449**, 3 (2007)
8. A. Zaritsky, S. Natan, E. Ben-Jacob, I. Tsarfaty, PLoS ONE **7**, e44671 (2012)
9. M. Poujade, E. Grasland-Mongrain, A. Hertzog, J. Jouanneau, P. Chavrier, B. Ladoux, A. Buguin, P. Silberzan, Proc. Natl. Acad. Sci. USA **104**, 15988 (2007)
10. M. Basan, J. Elgeti, E. Hannezo, W.-J. Rappel, H. Levine, Proc. Natl. Acad. Sci. USA **110**, 2452 (2013)
11. D.L. Nikolić, A.N. Boettiger, D. Bar-Sagi, J.D. Carbeck, S. Y. Shvartsman, Am. J. Physiol. - Cell Physiol. **291**, C68 (2006)
12. S. Sankararaman, S. Ramaswamy, Phys. Rev. Lett. **102**, 118107 (2009)
13. J.F. Joanny, S. Ramaswamy, J. Fluid Mech. **705**, 46 (2012)
14. N. Sarkara, A. Basu, The European Phys. J. E **35**, 115 (2012)
15. E. Khain, L.M. Sander, M. Scheider-Mizell, J. Stat. Phys. **128**, 209 (2007)
16. G. Forgacs, R.A Foty, Y. Shafrir, M.S. Steinberg, Biophys. J. **74**, 2227 (1998)
17. E.M. Schötz, R.D. Burdine, F. Jülicher, M.S. Steinberg, C.P. Heisenberg, R.A. Foty, HFSP J. **2**, 42 (2008)
18. R.A. Foty, G. Forgacs, C.M. Pfleger, M.S. Steinberg, Phys. Rev. Lett. **72**, 2298 (1994)
19. D.A. Kessler, J. Koplik, H. Levine, Phys. Rev. A **31**, 1712 (1985)
20. X. Trepat, M.R. Wasserman, T.E. Angelini, E. Millet, D.A. Weitz, J.P. Butler, J.J. Fredberg, Nat. Phys. **5**, 426 (2009)
21. N. Sepulveda, L. Petitjean, O. Cochet, E. Grasland-Mongrain, P. Silberzan, V. Hakim, PLOS Comput. Biol. **9**, e1002944 (2013)
22. S. Mark, R. Shlomovitz, N.S. Gov, M. Poujade, E. Grasland-Mongrain, P. Silberzan, Biophys. J. **98**, 361 (2010)